Multi-Way Partitioning of Power Networks via Koopman Mode Analysis

Fredrik Raak * **Yoshihiko Susuki** *,** **Takashi Hikihara** *

* *Kyoto University, Katsura, Nishikyo, Kyoto 615-8510, Japan (e-mail: f-raak@dove.kuee.kyoto-u.ac.jp).*
** *JST-CREST, 4-1-8 Honcho, Kawaguchi, Saitama 332-0012, Japan (e-mail: susuki@ieee.org).*

Abstract: This paper deals with the partitioning problem of power networks by applying the so-called Koopman Mode Analysis (KMA) to sampled voltage-angle data. KMA is based on the so-called Koopman operator defined for arbitrary nonlinear dynamical system and provides an infinite dimensional but linear description of the evolving nonlinear dynamics. By computing a set of dynamically relevant modes using the KMA, a new partitioning method for power networks is introduced, and multiple partitions are derived for a benchmark system. The obtained result is compared with two conventional methods previously applied to the partitioning problem; spectral graph theory and slow coherency.

Keywords: Power system monitoring, spectral graph theory, power network partitioning, coherency identification.

1. INTRODUCTION

A controlled islanding strategy aims to intentionally split a network into disjoint parts to prevent fault propagation in an emerging blackout scenario. The network partitioning problem is the key part of such a strategy. Partitioning a power network by means of coherent areas is also relevant for PMU placement and for deriving a simplified dynamic equivalence for a large network. Previously, numerous methods have been suggested to identify appropriate partitions. These methods are mainly based on one of two different approaches or a combination of them. The first approach is based on the notion of generator coherency which can be determined by a linearization of system equations. The second one is based on an analysis of the network structure (represented by a graph) to determine separation points by identifying clusters and weak connections between them. In this paper, as an alternative method, we aim to introduce a power network partitioning method based only on sampled data following a fault.

A popular analysis method for identification of coherent generators and areas is *Slow-Coherency* (SC) in Chow et al. (1995). In You et al. (2004) the SC method used in combination with a search algorithm to identify partitions intended for controlled islanding. An extended version of the classical SC method is derived in Yusof et al. (1993) to include all buses directly without restricting to generators' internal buses. Sun et al. (2003) outlines a method based on the so-called *ordered binary decision diagram* and evaluates it in a simulation study in Sun et al. (2005) and proposes a real-time strategy in Sun et al. (2006). Spectral graph theory is used in Ding et al. (2013) together with power flow and generator stability constraints and in Sanchez-Garcia et al. (2014) where they utilize a new dendrogram-based technique and evaluate different weights on edges (representing transmission lines) to construct the so-called graph Laplacian, from which partitions are derived through its eigenanalysis.

In this paper, we outline a power network partitioning method based on the Koopman Mode Analysis (KMA) applied to data on dynamics of voltage bus-angles sampled following a fault in a benchmark system. KMA was first introduced to power system analysis in Susuki and Mezić (2011) for coherency identification of generators and later used as a precursor to instability in Susuki and Mezić (2012). An overview of various applications of KMA and a comprehensive theoretical description is given in Budišić et al. (2012). Previously, KMA-based partitioning has been investigated by the current authors in Raak et al. (2014) and Raak et al. (2015). The contribution of this paper is to propose a new procedure for multi-way partitioning. The procedure is demonstrated by time-domain simulations with comparisons of partitioning using spectral graph theory and a slow coherency based method.

The remainder of this paper is organized as follows. Section 2 explains the fundamental concepts of KMA and gives a short description of spectral graph theory. Section 3 outlines the partitioning method applied in this paper. Section 4 presents simulation results of the method applied to a benchmark system. Finally, a summary and concluding remarks are given in Section 5.

Notation: The i-th component of a vector $\boldsymbol{v}$ is denoted $[\boldsymbol{v}]_i$. Likewise, the (i,j)-th entry of a matrix M is given by $[\mathsf{M}]_{ij}$. The euclidean norm of $\boldsymbol{v}$ is given by $\|\boldsymbol{v}\|$. A complex number z can be written as $z = A\angle\alpha$, where A is the modulus and α the argument. A set of integers with cardinality N is defined as $\mathcal{N} = \{1, \ldots, N\}$.

2. THEORETICAL BACKGROUNDS

2.1 Koopman Mode Analysis

The following theory is based on Budišić et al. (2012); Mezić (2005, 2013); Rowley et al. (2009); Susuki and Mezić (2011, 2012). Let us consider a continuous-time dynamical system evolving on a smooth manifold M ($\boldsymbol{x} \in M$):

$$\frac{d\boldsymbol{x}}{dt} = \boldsymbol{F}(\boldsymbol{x}), \tag{1}$$

where $\boldsymbol{x}$ contains the state variables of the system (such as generator angles and speeds in power system modeling) and $\boldsymbol{F}$ a function that governs the evolution. Since in this paper sampled dynamics are considered, the evolution (1) is rewritten as follows:

$$\boldsymbol{x}_{k+1} = \boldsymbol{\Phi}^h(\boldsymbol{x}_k), \quad h := t_{k+1} - t_k, \tag{2}$$

where $\boldsymbol{\Phi}^h$ is a mapping defined with solutions of (1) and h is the time-step between two consecutive samples. Now we introduce the so-called Koopman operator $\mathcal{U}$ and its fundamental characteristics. Consider a scalar observable $g : M \to \mathbb{R}$, such as a bus angle or voltage acquired via a measurement device in a power network. Applying $\mathcal{U}$ to g yields:

$$(\mathcal{U}g)(\boldsymbol{x}) := (g \circ \boldsymbol{\Phi}^h)(\boldsymbol{x}) = g(\boldsymbol{\Phi}^h(\boldsymbol{x})), \tag{3}$$

which is a composition of g with $\boldsymbol{\Phi}^h$. Since $\mathcal{U}$ is linear though infinite dimensional, its spectrum is expressed as

$$\mathcal{U}\varphi_i = \lambda_i \varphi_i, \quad i = 1, 2, \dots \tag{4}$$

where φ_i is the eigenfunction associated with the eigenvalue λ_i. Now, consider a vector observable $\boldsymbol{g} : M \to \mathbb{R}^m$. If all components of $\boldsymbol{g}$ lies within the span of φ_i, $\boldsymbol{g}$ can be decomposed in terms of an infinite sum:

$$\boldsymbol{g}(\boldsymbol{x}) = \sum_{i=1}^{\infty} \varphi_i(\boldsymbol{x}) \boldsymbol{v}_i, \tag{5}$$

where $\boldsymbol{v}_i$ is a vector coefficient associated with the pair (λ_i, φ_i) and called the Koopman Mode (KM). λ_i is called the Koopman Eigenvalue (KE). Applying $\mathcal{U}$ to (5) allows the evolution from $\boldsymbol{g}(\boldsymbol{x}_0)$ to $\boldsymbol{g}(\boldsymbol{x}_k)$ to be written as:

$$\boldsymbol{g}(\boldsymbol{x}_k) = \sum_{i=1}^{\infty} \varphi_i(\boldsymbol{x}_k) \boldsymbol{v}_i = \sum_{i=1}^{\infty} \lambda_i^k \varphi_i(\boldsymbol{x}_0) \boldsymbol{v}_i. \tag{6}$$

In Rowley et al. (2009), it is shown that an algorithm similar to the well known Arnoldi iteration produces the following decomposition of the same type as (6):

$$\left.\begin{aligned} \boldsymbol{g}_k &= \sum_{i=1}^{N} \tilde{\lambda}_i^k \tilde{\boldsymbol{v}}_i, \quad k = 0, \dots, N-1, \\ \boldsymbol{g}_N &= \sum_{i=1}^{N} \tilde{\lambda}_i^N \tilde{\boldsymbol{v}}_i + \boldsymbol{r}, \end{aligned}\right\} \tag{7}$$

where $\boldsymbol{r}$ is a residual term containing an approximation error. For $N+1$ vectors of measurements equally spaced in time, (7) approximates (6) in terms of a finite sum of N KMs and KEs. From now, when treating KMs and KEs, we will refer to pairs of *Ritz* vectors and values $(\tilde{\boldsymbol{v}}_i, \tilde{\lambda}_i)$. For a KM pair, the Growth Rate (GR) $|\tilde{\lambda}_i|$ is defined together with the norm $\|\tilde{\boldsymbol{v}}_i\|$, which are used to identify *dominant* KMs exhibiting sustained oscillations and large contributions to the sum (7).

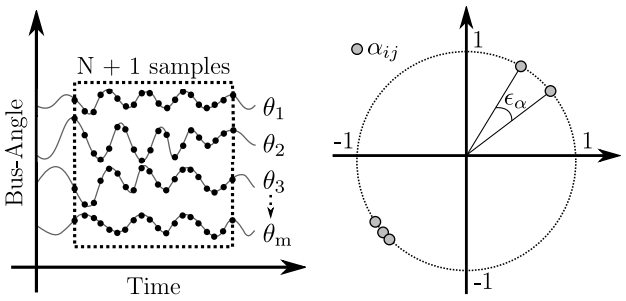

(a) Window of sampled data on bus-angles.

(b) Initial phases in a single KM plotted on the unit circle.

Fig. 1. Illustration of data acquisition in (a) and coherency of initial phase in (b).

Coherency identification for power network dynamics using KMs was originally proposed by Susuki and Mezić (2011). Suppose a set of KMs $\{\boldsymbol{v}_1, \dots, \boldsymbol{v}_N\}$ identified from a finite-time window of bus angle dynamics for a power network comprising m buses, see Fig. 1(a). First, consider the j-th element of the i-th KM, $[\boldsymbol{v}_i]_j = A_{ij} \angle \alpha_{ij}$, $i \in \mathcal{N}$, $j \in \{1, \dots, m\}$, where A_{ij} is called the *amplitude factor* and α_{ij} the *initial phase*. Naturally, in a *coherent group* of buses for a given KM $\boldsymbol{v}_i$, all buses are oscillating with a small phase difference between them. More rigorously, according to Budišić et al. (2012) by taking a positive constant ϵ_α, which we call the phase tolerance, and choosing two measurement points g_k and g_l from $\boldsymbol{g}$, we define the following condition for phase coherency:

$$|[\boldsymbol{\alpha}_i]_k - [\boldsymbol{\alpha}_i]_l| < \epsilon_\alpha, \tag{8}$$

where $\boldsymbol{\alpha}_i$ is the initial phase vector for $\boldsymbol{v}_i$. If (8) is fulfilled, then g_k and g_l are called ϵ_α-coherent for the i-th KM, see Fig. 1(b). When coherency for a collection of dominant KMs $\{\boldsymbol{v}_1, \dots, \boldsymbol{v}_d\}$ with associated initial phases $\mathsf{A}_\alpha := [\boldsymbol{\alpha}_1, \dots, \boldsymbol{\alpha}_d]$ is concerned, then (8) has to hold for all $\boldsymbol{\alpha}_i$ simultaneously which can be expressed as

$$|[\mathsf{A}_\alpha]_{ki} - [\mathsf{A}_\alpha]_{li}| < \epsilon_\alpha, \ \forall i \in \{1, \dots, d\}. \tag{9}$$

The coherency condition for multiple KMs given in (9) is exploited in the proposed multi-way partitioning.

2.2 Spectral Graph Theory

Spectral graph theory is the analysis of graphs (networks) by means of eigenvalues and eigenvectors of matrices associated with it, primarily the so-called Laplacian matrix. For a power network, buses are represented by vertices and transmission lines (and transformers) by edges. Connections of the network consisting of m buses are described by the adjacency matrix A where $[\mathsf{A}]_{ij} = [\mathsf{A}]_{ji} = w_{ji}$ if vertices $\{i, j\}$ are connected by an edge and $[\mathsf{A}]_{ij} = 0$ otherwise. Here, for edge weights, $w_{ji} = w_{ij}$ holds if unidirectional networks are considered. A network is concisely represented by the graph tuple $\mathcal{G} = (\mathcal{V}, \mathcal{E}, w)$, where $\mathcal{V}$ and $\mathcal{E}$ are the sets of vertices and edges. The degree of a vertex is defined as $d_i = \sum_{j=1}^{m} [\mathsf{A}]_{ij}$, i.e. the number of edges connected to each vertex. The graph Laplacian can then be defined as:

$$\mathsf{L} = \mathrm{diag}(d_i, \dots, d_m) - \mathsf{A}. \tag{10}$$

For connected networks, eigenvalues of (10) are listed based on increasing magnitude: $\lambda_1 = 0 < \lambda_2 < \cdots < \lambda_m$. On the other hand, a multiplicity of zeros implies that

Algorithm 1 Proposed partitioning via KMA

Require: $\{\boldsymbol{\theta}_0, \ldots, \boldsymbol{\theta}_N\}$: data set of bus-angle dynamics; $\mathcal{G} = (\mathcal{V}, \mathcal{E}, w)$: graph of the target power network
Ensure: Cutset
1: $\{(\tilde{\lambda}_i, \tilde{\boldsymbol{v}}_i); i \in \mathcal{N}\} \leftarrow \text{RunKMA}(\Theta)$
2: $\mathcal{N}_\text{d} \subseteq \mathcal{N} \leftarrow \text{DominantKMs}(\tilde{\lambda}, \tilde{\boldsymbol{v}})$
3: $\{\boldsymbol{\alpha}_i; i \in \mathcal{N}_\text{d}\} \leftarrow \text{IntialPhaseVector}(\tilde{\boldsymbol{v}}, \mathcal{N}_\text{d})$
4: $\mathsf{C}_\text{G} = [\boldsymbol{c}_1, \ldots, \boldsymbol{c}_\text{NCG}] \leftarrow \text{DetermineNCG}(\boldsymbol{\alpha}_i; i \in \mathcal{N}_\text{d})$
5: $\text{IdentifyCutset}(\mathsf{C}_\text{G}, \mathcal{G})$

the network consists of a number of disjoint sub-networks corresponding exactly to the number of zero eigenvalues. The eigenvector $\boldsymbol{V}_2$, associated with λ_2, the second smallest eigenvalue of a connected network, is of essential importance in the partitioning of a network. A 2-way partitioning, in other words the *graph bisectioning*, can be determined by evaluating the sign of each component in $\boldsymbol{V}_2$ as follows:

$$i \in \mathcal{V}_1 \;\text{ if }\; [\boldsymbol{V}_2]_i \geq 0, \quad i \in \mathcal{V}_2 \;\text{ if }\; [\boldsymbol{V}_2]_i < 0, \tag{11}$$

where $\mathcal{V}_1$ and $\mathcal{V}_2$ are the two disjoint sets of vertices. For a multilevel partitioning using eigenvectors, we can consider two simple approaches. The first one is to apply (11) iteratively on the increasingly smaller partitions until a desired amount of partitions is obtained. The second one described in Riolo and Newman (2012) is to consider a matrix $\mathsf{W} := [\boldsymbol{V}_2, \ldots, \boldsymbol{V}_{k>2}]$, where the rows of W can be interpreted as points in a $(k-1)$-dimensional space. One can now apply a k-means clustering method, see Kanungo et al. (2002), to obtain k partitions.

3. KMA-BASED PARTITIONING METHOD

In difference to conventional methods, the proposed partitioning method is solely based on information extracted from a dataset of sampled dynamics and is intended to capture the actual dynamic behavior of the system following a fault. Consider bus-angle dynamics acquired under uniform sampling:

$$\{\boldsymbol{\theta}_0, \ldots, \boldsymbol{\theta}_N\}, \tag{12}$$

where $\boldsymbol{\theta} = [\theta_i, \ldots, \theta_m]^\top$ and the subscript in (12) corresponds to an instance in time. Furthermore, the following two assumptions are made:

(i) Bus-angle data for every bus is acquired.
(ii) Structure of the network is known.

Assumptions (i) and (ii) are reasonable since the method is intended to the backbone high-voltage transmission system which does not generally comprise more buses than in the order hundreds: see Sun et al. (2005). Partitions are identified from a single KM and combination of multiple KMs by the following steps in Algorithm 1:

(1) Applying KMA to (12) gives N KMs (RunKMA).
(2) Sort and list all KMs based on decreasing GR and select typically the 20-30 KMs with the largest GRs. Among those KMs, limit the selection to KMs with the largest norms (in this paper we have chosen 9 including 8 oscillatory pairs). In this manner, KMs likely to represent the dynamical information in the set of data have been identified. These are the dominant KMs and identified as the set $\mathcal{N}_\text{d} \subseteq \mathcal{N}$ (DominantKMs).

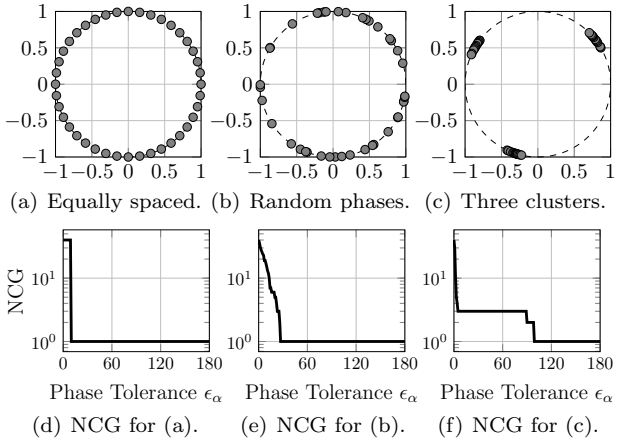

(a) Equally spaced. (b) Random phases. (c) Three clusters.
(d) NCG for (a). (e) NCG for (b). (f) NCG for (c).

Fig. 2. Illustrative examples of how the Number of Coherent Groups (NCG) varies as a function of phase tolerance ϵ_α. The number of phase points (and maximal NCG) is 40, (a) shows uniformly distributed angles with 9° phase difference between two consecutive points, (b) uniformly distributed random angles $[0°, 360°]$, and (c) three clear clusters of phase points. Plots (d)-(f) show NCG when ϵ_α is varied from 0° to 120° for the phase distribution given directly above.

(3) Initial phase vectors are calculated (IntialPhaseVector).
(4) Through the use of (8), important information can be gathered for how the Number of Coherent Groups (NCG) varies with the chosen tolerance ϵ_α as illustrated in Fig. 2. A large phase tolerance span for for a certain NCG is indicative of a clear separation between clusters of buses. An appropriate grouping in terms of multiple KMs can be derived by means of (9). A grouping matrix $\mathsf{C}_\text{G} = [\boldsymbol{c}_1, \ldots, \boldsymbol{c}_\text{NCG}]$ containing the coherent groups is identified (DetermineNCG).
(5) With C_G determined, the cutsets are simply identified by finding the transmission lines connecting buses belonging to different groups (IdentifyCutset).

Figure 2 shows an example of identification of coherent groups based on the condition (8) as a function of the phase tolerance ϵ_α. If phase angles are distributed equally with a fixed spacing (9° is used in Fig. 2(a)), then obviously NCG decreases from the number of phase angles to 1 when $\epsilon_\alpha = 10°$. Let $\epsilon_{\text{m}\alpha}$ denote the minimum angle difference between two points such that $\text{NCG}(\epsilon_{\text{m}\alpha} + \epsilon) = 1$, where ϵ is a small, positive constant ($\epsilon_{\text{m}\alpha} = 9°$ for Fig. 2(a)). For the randomly distributed set of phase angles in Fig. 2(b), NCG decreases from its maximal value until $\text{NCG}(\epsilon_{\text{m}\alpha})$ in a linear manner on the logarithmic plot, which corresponds to an exponential decrease. On the other hand, for a clustered phase angle distribution (Figs. 2(c) and (f)), a large permissiveness to changes in ϵ_α visible as constant plateaus is evident. Thus, the coherent groups for KMs are identified by locating the plateaus.

4. DEMONSTRATION

4.1 Benchmark System and Simulation Setting

The IEEE 118-bus test system in Fig. 3 is adopted as a benchmark system with load-flow data acquired from the

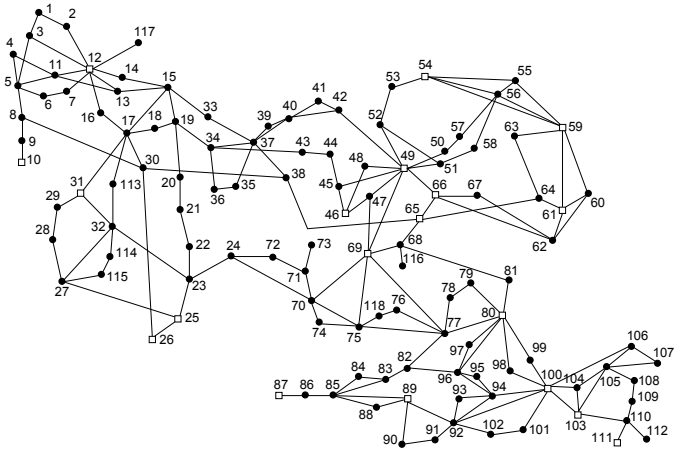

Fig. 3. IEEE 118-bus test system. Dynamics of the system are simulated with the classical model of 19 generators. Generator buses are indicated by hollow squares, and load and intermediate buses by filled circles.

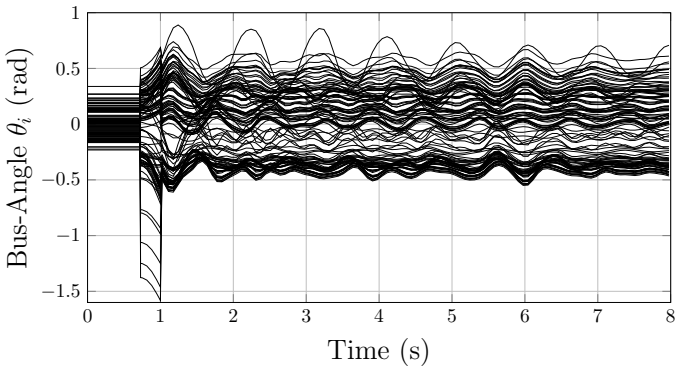

Fig. 4. Dynamics of bus-angles in the IEEE 118-bus test system following a three-phase fault at bus 17 (the same data are also used in Raak et al. (2015)).

Power Systems Test Case Archive (accessed on February 9, 2015) and simulated with 19 synchronous generators with parameters chosen same as Sun et al. (2005). Simulations are carried out using the Power System Analysis Toolbox (PSAT) for MATLAB, see Milano (2005).

Every bus-angle measurement is related to a mean-angle defined at a time-instant $k = t_k$ as

$$\bar{\theta}_k := \frac{1}{m}\sum_{j=1}^{m}\theta_{j,k}, \tag{13}$$

which acts as a reference frame similar to the center of inertia or center of angle defined for generator rotor angles, see Kundur (1994). The advantage of the choice is that we do not need any additional generator measurements to establish a reference. By relating each bus-angle to the mean angle, it is easy to detect the coherent motions of groups of buses swinging against each other or separating the system in a desynchronized manner.

In the proposed partitioning method, to facilitate clear results with few and large coherent groups and to prevent the case where scattered isolated buses becomes identified as partition candidates, we disregard "lonely" buses with a phase difference more than $\epsilon_\alpha \pm 10°$ to its closest neighbor and let those buses join its closest geographical neighbor.

Table 1. Dominant KMs obtained for the data on bus-angle dynamics shown in Fig. 4.

No. j	GR $\lvert\tilde{\lambda}_j\rvert$	Freq. [Hz] $\mathrm{Im}[\ln\tilde{\lambda}_j]/(2\pi T_s)$	Norm $\lVert\tilde{\boldsymbol{v}}_j\rVert$
1	1	0	3.29
2	0.9977	$\pm$1.04	0.28
3	0.9976	$\pm$1.24	0.25
⋮	0.9975	$\pm$3.29	0.05
⋮	0.9970	$\pm$0.21	0.02
⋮	0.9965	$\pm$2.59	0.03
⋮	0.9959	$\pm$2.37	0.16
4	0.9950	$\pm$2.02	0.19

4.2 Partitioning Results

The test system is subjected to a three-phase fault at bus 17 inducing the oscillatory response shown in Fig. 4. The short-circuit duration is 280 ms and is cleared at $t = 1$ s. KMA is now applied to the data for [1,8] s with a $f_s = 1/T_s = 60$ Hz sampling frequency which yields 420 KMs. Dominant KMs are identified and listed in Table 1. Let us here pick up the three oscillatory KMs which rows are marked in gray, because of their large norms compared to the rest. KM-1 is a bias mode containing a time-average of bus-angle measurements and is hence not used for the partitioning. In Fig. 5, initial phases for the chosen KMs are plotted on the unit circle. A few scattered buses are clearly visible in Fig. 5 (one for KM-3 and three for KM-4) and are here disregarded as explained in the previous section.

Figure 6 presents NCG vs. ϵ_α plots for the three KMs individually and for their combination based on (9). KM-2 displays a clear partitioning for two groups which is maintained for $\epsilon_\alpha \in [5°, 152°]$, and KM-4 gives a similar result. KM-3 displays clear plateaus for a NCG of 4,3 and 2. For the plot corresponding to NCG for multiple KMs denoted "All KMs," a wide plateau is visible for NCG = 4. However, for this plateau NCG decreases to 1 for KM-4 and does not provide any information. Thus, the second largest plateau occurring for NCG = 5 is used here as a multi-way partitioning for KMs. This actually corresponds to the union of cutsets for NCG = 2 for all KMs, shown in Fig. 7. The almost identical cutsets (except for the two load-buses 71 and 73) in the left central part provided by KM-3 and 4 are treated as one which ultimately provides a 4-way partitioning of the network.

The KMA-based partitioning is depicted in the benchmark system in Fig. 8. For the sake of comparison, a 4-way SC partitioning derived with the technique in Yusof et al. (1993) and lastly, 3 and 4-way partitioning using the Laplacian eigenvectors $\{\boldsymbol{V}_2,\boldsymbol{V}_3\}$ and $\{\boldsymbol{V}_2,\boldsymbol{V}_3,\boldsymbol{V}_4\}$, together with k-means are also illustrated in Fig. 8. The Laplacian is produced with all edge weights w_{ij} set to 1.

Let us compare the 4-way partitioning results. Roughly speaking, the three different techniques identify the same three large partitions. The KMA and SC based methods identify a coherent area around generator bus 87. In fact, the resulting partitions contain the same generators. On the contrary, graph-based partitioning suggests a partition in the lower right part of the network.

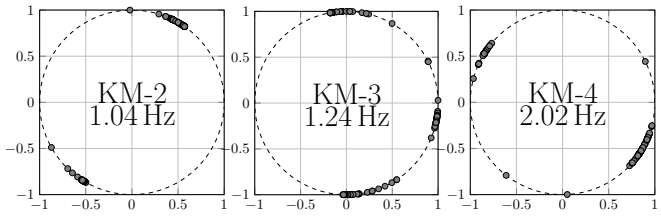

Fig. 5. Initial phases for KMs 2-4 given in Table 1 plotted on the unit circle (plots also appear in Raak et al. (2015)).

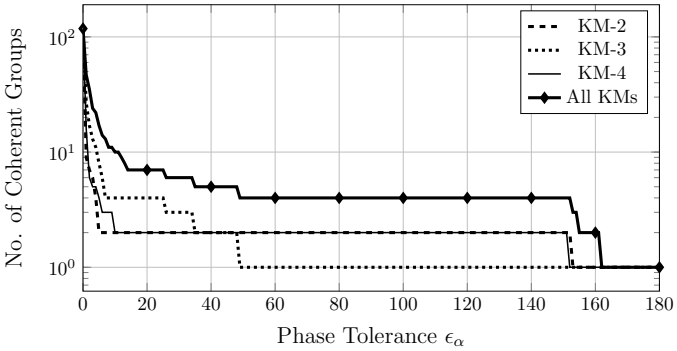

Fig. 6. Number of Coherent Groups (NCG) vs. phase tolerance ϵ_α according to (8) for KMs 2-4 and for the combination of them ("All KMs").

4.3 Time-Domain Simulations

Now time-domain simulations are run for the four different partitioning results in Fig. 8. The system remains in a steady state until $t = 1$ s when the network separation is initiated by simultaneously disconnecting all tie-lines associated with the partitioning. In Fig. 9, time responses for angular frequencies ω_i of generators are given for the four cases. It is clear that all simulation cases yield stable responses converging to new steady states. The magnitude of the frequency deviation depends on the balance between load and generation, and the lowest deviations are achieved for the partitioning according to spectral graph theory into three parts. For 4-way partitioning, the proposed KMA-based method yields the overall smallest frequency deviations.

A close up showing the angular responses of generators during the first second after separation are given in Fig. 10. The KMA-based partitioning displays possibly the smallest oscillation amplitudes of generators for 4-way partitioning.

5. CONCLUDING REMARKS

In this paper, we proposed and demonstrated a method of power network partitioning based solely on measurements of bus voltage angles by applying the so-called Koopman Mode Analysis (KMA). The KMA-based method was applied to the IEEE 118-bus test system and the result was compared with two other well-known methods of network partitioning; spectral graph theory and a technique based on slow coherency. By exploiting a new coherency condition in (9) for KMs based on a maximum allowable phase difference tolerance between two buses, an appropriate amount of partitions can be identified as

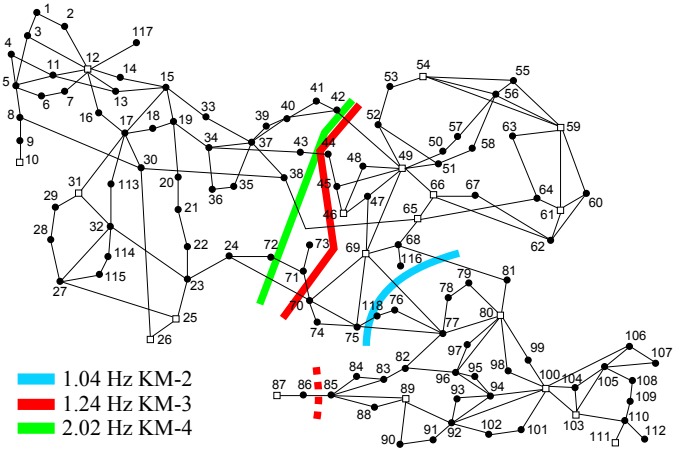

Fig. 7. Partitioning of the benchmark system for KMs 2-4 with cutsets indicated by colored lines.

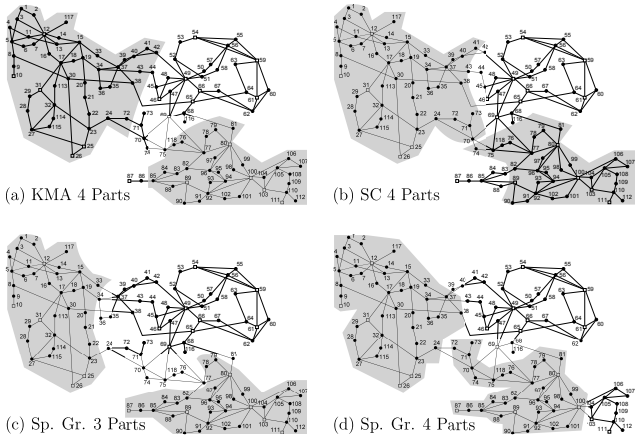

Fig. 8. Multi-way partitioning of the IEEE 118-bus test system based on (a) phase-coherency in KMs 2-4 identified from dynamics of the three phase fault, (b) a Slow-Coherency (SC) technique including load buses, and (c)-(d) for spectral graph theory for 3 and 4-way partitioning. Disjoint partitions can be distinguished based on the gray and non-colored areas.

a permissiveness to changes in phase difference tolerance for a certain Number of Coherent Groups (NCG), which is apparent as plateaus in a NCG vs. phase tolerance plot. This technique is valid for multiple KMs and can thus derive multiple frequency coherent partitions.

REFERENCES

Budišić, M., Mohr, R., and Mezić, I. (2012). Applied Koopmanism. *Chaos*, 22(4).

Chow, J.H., Galarza, R., Accari, P., and Price, W.W. (1995). Inertial and slow coherency aggregation algorithms for power system dynamic model reduction. *IEEE Transactions on Power Systems*, 10(2), 680–685.

Ding, L., Gonzalez-Longatt, F., Wall, P., and Terzija, V. (2013). Two-step spectral clustering controlled islanding algorithm. *IEEE Transactions on Power Systems*, 28(1), 75–84.

Kanungo, T., Mount, D.M., Netanyahu, N.S., Piatko, C.D., Silverman, R., and Wu, A.Y. (2002). An efficient k-means clustering algorithms: Analysis and implemen-

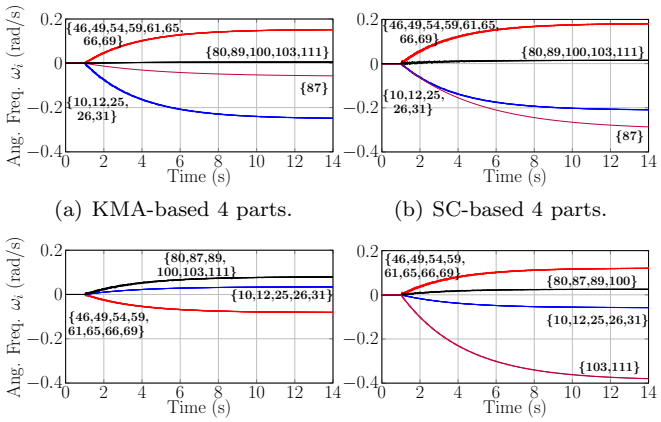

(a) KMA-based 4 parts. (b) SC-based 4 parts.

(c) Spectral graph 3 parts. (d) Spectral graph 4 parts.

Fig. 9. Rotor speed dynamics (deviation from steady state is shown) for time-domain simulations of islanding operation initiated at $t = 1$ s for the four different sets of partitioning in Fig 8. Rotor speeds for generators belonging to the same group are plotted in the same color and their bus numbers are given inside of the brackets.

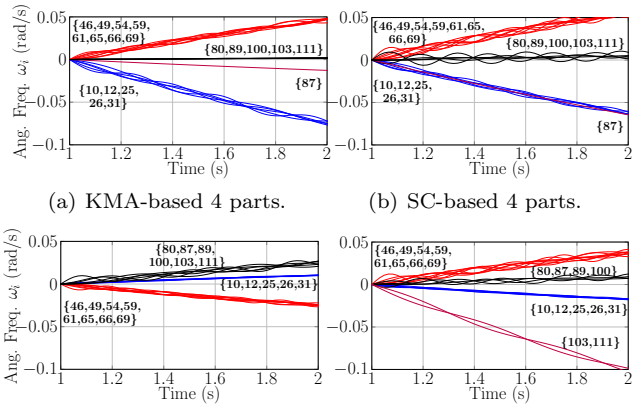

(a) KMA-based 4 parts. (b) SC-based 4 parts.

(c) Spectral graph 3 parts. (d) Spectral graph 4 parts.

Fig. 10. Same data as in Fig. 9 shown for the first second following the islanding operation.

tation. *IEEE Transactions on Pattern Analysis and Machine Intelligence*, 24(7), 881–892.

Kundur, P. (1994). *Power System Stability and Control*. McGraw-Hill.

Mezić, I. (2005). Spectral properties of dynamical systems, model reduction and decompositions. *Nonlinear Dynamics*, 41(1-3), 309–325.

Mezić, I. (2013). Analysis of fluid flows via spectral properties of the Koopman operator. *Annual Review of Fluid Mechanics*, 45, 357–378.

Milano, F. (2005). An open source power system analysis toolbox. *IEEE Transactions on Power Systems*, 20(3), 1199–1206.

Power Systems Test Case Archive (Accessed February 9, 2015). College of Engineering, University of Washington. [Online]. Available: `http://www.ee.washington.edu/research/pstca/`.

Raak, F., Susuki, Y., and Hikihara, T. (2015). Data-driven partitioning of power networks via Koopman mode analysis. In revision.

Raak, F., Susuki, Y., Hikihara, T., Chamorro, H.R., and Ghandhari, M. (2014). Partitioning power grids via nonlinear Koopman mode analysis. In *Innovative Smart Grid Technologies Conference (ISGT), 2014 IEEE PES*, 1–5.

Riolo, M.A. and Newman, M.E.J. (2012). First-principles multiway spectral partitioning of graphs. *CoRR*, abs/1209.5969.

Rowley, C.W., Mezić, I., Bagheri, S., Schlatter, P., and Henningson, D.S. (2009). Spectral analysis of nonlinear flows. *Journal of Fluid Mechanics*, 641, 115–127.

Sanchez-Garcia, R., Fennelly, M., Norris, S., Wright, N., Niblo, G., Brodzki, J., and Bialek, J. (2014). Hierarchical spectral clustering of power grids. *IEEE Transactions on Power Systems*.

Sun, K., Zheng, D.., and Lu, Q. (2003). Splitting strategies for islanding operation of large-scale power systems using OBDD-based methods. *IEEE Transactions on Power Systems*, 18(2), 912–923.

Sun, K., Zheng, D.., and Lu, Q. (2005). A simulation study of OBDD-based proper splitting strategies for power systems under consideration of transient stability. *IEEE Transactions on Power Systems*, 20(1), 389–399.

Sun, K., Zheng, D.Z., and Lu, Q. (2006). Searching for feasible splitting strategies of controlled system islanding. *IEE Proceedings: Generation, Transmission and Distribution*, 153(1), 89–98.

Susuki, Y. and Mezić, I. (2011). Nonlinear Koopman modes and coherency identification of coupled swing dynamics. *IEEE Transactions on Power Systems*, 26(4), 1894–1904. Also, correction, *this journal*, vol. 26, no. 4, p. 2584, 2011.

Susuki, Y. and Mezić, I. (2012). Nonlinear Koopman modes and a precursor to power system swing instabilities. *IEEE Transactions on Power Systems*, 27(3), 1182–1191.

You, H., Vittal, V., and Wang, X. (2004). Slow coherency-based islanding. *IEEE Transactions on Power Systems*, 19(1), 483–491.

Yusof, S., Rogers, G., and Alden, R. (1993). Slow coherency based network partitioning including load buses. *IEEE Transactions on Power Systems*, 8(3), 1375–1381.